Using spectral reflectance to estimate leaf chlorophyll content of tea with shading treatments

Title

Using spectral reflectance to estimate leaf chlorophyll content of tea with shading treatments

Author names and affiliations

Rei Sonobe[a], Tomohito Sano[b] and Hideki Horie[c]

[a] Faculty of Agriculture, Shizuoka University, 836 Ohya, Suruga-ku, Shizuoka, 422-8529, Japan

[b]Headquarters, National Agriculture and Food Research Organization, 3-1-1 Kannondai, Tsukuba, Ibaraki 305-8517, Japan

[c]Institute of Fruit Tree and Tea Science, National Agriculture and Food Research Organization, 2769 Shishidoi, Kanaya, Shimada, Shizuoka 428-8501, Japan

Corresponding author

Rei Sonobe

reysnb@gmail.com

Abstract

Some stresses are utilised to improve qualities of agricultural products. Low light stress increases the chlorophyll content of tea leaves, which improves appearance. Although chlorophyll content estimation is one of the most common applications of hyperspectral remote sensing, previous studies were based on measurements under relatively low stress conditions. In this study, two methods, machine learning algorithms and the inversion of a radiative transfer model, were evaluated using measurements from tea leaves with shading treatments. According to the ratio of performance to deviation (RPD), PROSPECT-D inversion (RPD=1.71-2.31) had the potential for quantifying chlorophyll content; although, it required some improvements. Overall, the regression models based on machine learning had high performances. The kernel-based extreme learning machine had the highest performance with a root mean square error of 3.04 ± 0.52 μg cm^{-2} and RPD values from 3.38 to 5.92 for the test set, which was used for assessing generalisation error.

Keywords: chlorophyll; green tea; vegetation indices; machine learning; PROSPECT-D

1. Introduction

Green tea is a very healthy beverage because its consumption is associated with reduced mortality, and it has attracted a great deal of attention (Kuriyama *et al.* 2006). Green tea-flavoured sweets have even become popular. Some techniques have been developed for increasing chlorophyll content, which is important for improving tea leaf appearance. Chlorophyll content is strongly related to the colour of dry tea leaves (Wang *et al.* 2004) and the flavour of tea is principally determined by chemical components. Chlorophyll content is positively correlated with the total quality score as well as the scores for appearance and infused leaf (Wang *et al.* 2010). Therefore, various methods are used to increase the chlorophyll content of tea leaves during growth (Lee *et al.* 2013). The control of light transmission by shade treatment is the most effective method for increasing chlorophyll content in tea plants (De Costa *et al.* 2007) and shading nets (70–95% shading) have been used in Shizuoka, Japan to increase the chlorophyll content of tea leaves and to improve appearance (Sonobe *et al.* 2018a). However, excessive shading tea can lead to early mortalities due to the excessive environmental stresses caused by reducing natural photosynthesis in the leaves. Both quantifying chlorophyll contents and detecting environmental stresses using field measurements are required for better tea tree management, and no applicable approach has been established.

As destructive methods, spectrophotometric measurements using ultraviolet and visible (UV-VIS) spectroscopy and high-performance liquid chromatography (HPLC) measurements have been used to quantify pigment content in leaves (Prado-Cabrero *et al.* 2016). However, these techniques are expensive, labour-intensive and not always applicable for in-situ measurements. Alternately, the SPAD-502 Leaf Chlorophyll Meter (Konica Minolta Inc.) has been used for field measurements of leaf chlorophyll content (le Maire *et al.* 2004; Elarab *et al.* 2015). However, light intensity also influences leaf thickness (Murchie *et al.* 2005) and that makes the output of the meter obscure (Yamamoto *et al.* 2002). In contrast, remote sensing using hyperspectral reflectance has been used to evaluate biochemical properties (Whetton *et al.* 2018), especially chlorophyll content estimation, which has received special attention since chlorophyll pigments closely relate to protective activity against a variety of degenerative diseases as well as the photosynthetic process (Korus 2013). Furthermore, because remote sensing is a non-destructive method that can cover large areas and reflect the spatial variability of crop canopies using sensors mounted on airborne drones or satellites, this technique is useful for improving fertiliser management (Gabriel *et al.* 2017).

The numerical inversion of radiative transfer models (RTMs) has been proposed to estimate chlorophyll content using hyperspectral remote sensing (Li *et al.* 2015; Masemola *et al.* 2016). PROpriétés SPECTrales (PROSPECT) is one of the most famous RTMs and has been widely used to assess the biochemical properties of broadleaf species and herbs (Jacquemoud *et al.* 1996; Féret *et al.* 2008; Hernandez-Clemente *et al.* 2014; Sonobe *et al.* 2018b; Sun *et al.* 2018). The latest version, PROSPECT-D, has an improved ability to estimate pigment content (Féret *et al.* 2017). Although le Maire et al. (2004) pointed out that the previous versions of PROSPECT were not accurate enough to evaluate broad leaf chlorophyll content, this version has not been fully evaluated.

Another recent option for estimating chlorophyll content from hyperspectral reflectance is based on machine learning algorithms (Liang *et al.* 2016; Chemura *et al.* 2017). Random forests (RF) is specifically mentioned as a successful classification and regression method (Biau and Scornet 2016), and has been widely used for evaluating the aboveground biomass of C3 and C4 grasses (Shoko *et al.* 2018). Support vector machine (SVM) has also been a very effective approach and is appropriate to express the relationship between reflectance and leaf water status (Das *et al.* 2017).

In addition, the high performances of kernel-based extreme learning machine (KELM) have been shown in some previous studies for solving regression problems (Sonobe et al., 2018a). Therefore, the machine learning algorithms RF, SVM and KELM were applied to estimate the chlorophyll content of shade grown tea from hyperspectral reflectance. Notably, the disadvantages of machine learning algorithms are that they require training data for prediction and not enough training data leads to overfitting and the models could be unsuitable. In this study, the machine learning algorithms which possess only two hyperparameters were evaluated.

Vegetation indices have also been widely used to emphasise the features of vegetation (Sonobe *et al.* 2018c) and a number of vegetation indices have been developed for evaluating chlorophyll content. Most vegetation indices for chlorophyll content are based on wavelengths ranging from 400 to 860 nm, which covers photosynthetically active radiation. There are reflectance value or derivative-based indices and feature-based indices, mainly on the properties of the red edge. However, most indices are only applicable to the specific species or specific leaf types, such as sunlit or shaded leaves, from which they were developed (Sonobe and Wang 2017a). In this study, regression models using vegetation indices were evaluated as well as regression models based on original reflectance and their accuracies were compared.

In leaves, there are two types of chlorophyll pigments (chlorophyll a and b) and the chlorophyll a/b ratio is positively correlated with the ratio of photosystem II cores to light harvesting chlorophyll-protein complex (Terashima and Hikosaka 1995). As a result, the cultivation using shading treatments imposes environmental stress on vegetation and changes the balance among chlorophyll a and b contents. However, some previous studies have used datasets composed of measurements taken under relatively low light-stress conditions (e.g. the coefficients of linear regression models for estimating chlorophyll a content from carotenoid content were 2.99 (Hosgood *et al.* 1994) to 3.45 (Féret *et al.* 2008)). Therefore, some approaches in previous studies for estimating chlorophyll content are not valid for evaluating the chlorophyll content of shade grown tea, and these approaches were evaluated in this study.

The objective of this study was to examine the potential of hyperspectral remote sensing approaches including radiative transfer model inversion and machine learning algorithms for quantifying chlorophyll content of tea that was grown under low-light stress.

2. Materials and methods

2.1. Measurements and datasets

The first flush of leaves, which are harvested from mid-April to mid-May, have the highest quality and, therefore, we focused on this period. The experiments were conducted at the Institute of Fruit Tree and Tea Science, National Agriculture and Food Research Organization, Shimada, Japan. Daily temperatures and precipitation varied between 12.5–19.2 °C and 0–17.5 mm, respectively, during the experiment (Japan Meteorological Agency, 2017). Four shading treatments were conducted using no net (0% shading), shading net #410 (35% shading), #1210 (75% shading) and #1220 (90% shading) (Dio Chemicals, Ltd., Japan) to assess the influence of shading on tea chlorophyll content from 21 April 2017 to 11 May 2017.

Forty-six samples (8 samples for 0% shading, 12 samples for 35% shading, 12 samples for 75%

shading and 14 samples for 90% shading) and 60 measurements (15 samples for each treatment) were collected on 1 and 11 May 2017, respectively. After sampling, we used the spectral reflectance and biochemical properties including chlorophyll a, b and carotenoid content for 106 leaf samples.

A spectrometer (FieldSpec4, Analytical Spectral Devices Inc., USA) with three detectors (VNIR, SWIR 1 and SWIR 2) was used to obtain reflectance data with a leaf clip. The drifts depended on some inherent variation in detector sensitivities and were confirmed at these connections (i.e. the wavelengths of 1000 and 1800 nm). Thus, the splice correction function was applied to modify these connections using ViewSpec Pro Software (Analytical Spectral Devices Inc., USA).

Leaf discs were used for pigment concentration measurements in dimethyl-formamide extracts using dual-beam scanning ultraviolet-visible spectrophotometers (UV-1280, Shimadzu, Japan). The following equations were used to quantify chlorophyll content (Wellburn 1994):

$$\text{Chlorophyll} = \text{Chlorophyll a} + \text{Chlorophyll b} \qquad (1)$$

$$\text{Chlorophyll a} = 12A_{663.8} - 3.11A_{646.8} \qquad (2)$$

$$\text{Chlorophyll b} = 20.78A_{646.8} - 4.88A_{663.8} \qquad (3)$$

where A is the absorbance and the subscripts are the wavelength (nm).

2.2. Vegetation indices

Vegetation indices calculated from various remote sensing sensors are effective for removing variability caused by other features, such as soil background and atmospheric conditions

(Blackburn and Steele 1999). They are also effecting for reducing the data saturation problem (Mutanga and Skidmore 2004) and in quantitative and qualitative evaluations of vegetation cover, vigour and growth dynamics, among other applications, that are important components of precision agriculture (Panda *et al.* 2010). Many studies have focused on chlorophyll content estimation based on hyperspectral remote sensing techniques, and a number of vegetation indices have been developed for this purpose. In this study, 96 published vegetation indices (Table 1) were used as inputs of machine learning models for estimating the chlorophyll content of shaded tea. Five (i.e. Chl_{green}, $Chl_{red\ edge}1$, $Chl_{red\ edge}2$, chlorophyll vegetation index (CVI) and global imager vegetation index (GLI)) are based on broadband reflectance and the mean reflectance values were used in this study. Although most of the indices are based on original reflectance or a first derivative at a given wavelength ($R_{wavelength}$ or $D_{wavelength}$), there are eight feature-based indices that focus on the red edge (i.e. edge-green first derivative normalized difference (EGFN), edge-green first derivative ratio (EGFR), wavelength of the red edge (RE), Red-Edge Inflection Point (REIP), Red-edge position liner extrapolation method proposed by Cho and Skidmore (2006) (REP1), Red-edge position liner extrapolation method proposed by Guyot and Baret (1988) (REP2), sum of the amplitudes between 680 and 780 nm in the first derivative of the reflectance spectra (Sum1) and sum of derivative values between 626 nm and 795 nm (Sum2)). They are calculated as a sum value of the reflectance (Elvidge and Chen 1995; Filella *et al.* 1995) or a wavelength value (Collins 1978; Horler *et al.* 1983; Miller *et al.* 1990; Filella *et al.* 1995). In addition, the triangular vegetation index (TVI) (Broge and Leblanc 2001) and spectral polygon vegetation index (SPVI) (Vincini *et al.* 2006) are categorised as feature-based indices.

The indices based on original reflectance or first derivative are divided into four groups: reflectance or first derivative at a given wavelength or inverse reflectance (R, D or 1/R) (Boochs *et al.* 1990; Gitelson *et al.* 1999; Carter and Knapp 2001); difference in reflectance (DR) (Jordan 1969; Buschmann and Nagel 1993); simple ratio (SR) (Jordan 1969; Chappelle *et al.* 1992; Vogelmann *et al.* 1993; Carter 1994; McMurtrey *et al.* 1994; Peñuelas *et al.* 1995a; Gitelson and Merzlyak 1996; Lichtenthaler *et al.* 1996; Zarco-Tejada *et al.* 2003a; Zarco-Tejada *et al.* 2003c; Delalieux *et al.* 2009; Gong *et al.* 2014) or modified simple ratio (mSR) (Sims and Gamon 2002); and normalized differences (ND or dND) (Gong *et al.* 2014; Sonobe and Wang 2018; Sonobe and Wang 2017b). In addition, complicated indices based on soil line (Rondeaux *et al.* 1996; Wu *et al.* 2008), chlorophyll absorption ratio indices (Kim *et al.* 1994; Daughtry *et al.* 2000; Wu *et al.* 2008; Guan and Liu 2009) and integrated forms (Daughtry *et al.* 2000; Wu *et al.* 2008; Guan and Liu 2009) were evaluated in this study.

<Table 1>

2.3. Regression models based on machine learning algorithms

Machine learning algorithms including random forests (RF), support vector machine (SVM) and kernel-based extreme learning machine (KELM) were applied to estimate the chlorophyll content of shade grown tea from hyperspectral reflectance.

The optimisations of each machine learning algorithm were conducted based on Bayesian optimisation, which is a framework used to optimise hyperparameters of noisy, expansive black-box functions and it defines a principled approach to modelling uncertainty (Bergstra and Bengio 2012). These processes were conducted with the Gaussian process (GP), which is a continuous stochastic process commonly used for Bayesian optimisation (Snoek *et al.* 2015). All the processes were conducted using R 3.4.3 (R Core Team 2017). While KELM was conducted using MATLAB and Statistics Toolbox Release 2016a (MathWorks, Inc., USA) and the source code was downloaded from http://www.ntu.edu.sg/home/egbhuang/index.html, RF and SVM were assessed using the 'randomForest' package (Liaw and Wiener 2002) and 'kernlab' package (Karatzoglou *et al.* 2004), respectively. For applying Bayesian optimisation, the ‘rBayesianOptimization’ package (Yan 2016) was applied.

2.3.1 Random forests

RF is an ensemble learning technique that builds multiple trees (the classification and regression tree, CART) (Breiman 2001) and its two user-defined parameters, number of trees (ntree) and the number of variables used to split the nodes (mtry), are normally optimised. Each tree is built using training data and the nodes are split using the best split variable out of a group of randomly selected variables (Liaw and Wiener 2002). This strategy guards against over-fitting and can handle thousands of dependent and independent input variables without variable deletion. Although the two main user-defined parameters are the number of trees (k) and the number of variables used to split the nodes (m), the generalisation error always converges, and overfitting is not a problem if the number of trees is increased. However, randomising the splitting rule can improve the performance for ensembles (Ishwaran 2015; Sonobe *et al.* 2017). Therefore, three hyperparameters including the minimum number of unique cases in a terminal node (nodesize), the maximum depth to which a tree should be grown (nodedepth) and the number of random splits (nsplit) were optimised in this study, as well as ntree and mtry.

2.3.2 Support vector machine

SVM has been successfully applied to solve the problem of high dimension and local minima (Ding *et al.* 2016). The 'kernel trick' has frequently been applied instead of attempting to fit a non-linear model in previous studies for classification and regression, and the Gaussian Radial Basis Function (RBF) kernel was most used (Chatziantoniou *et al.* 2017). In this study, the RBF kernel was applied, and the regularisation parameter C and the kernel bandwidth σ were tuned to control the flexibility.

2.3.3 Kernel based extreme learning machine

ELM (Huang *et al.* 2006), which is expressed as a single hidden layer feed-forward neural network, has been widely applied for many practical tasks, such as prediction, fault diagnosis, recognition, classification and signal processing (Li *et al.* 2016). Since a fixed hidden layer is composed of a vast number of nonlinear nodes and the hidden layer bias is defined randomly in this algorithm (Huang *et al.* 2006), it possesses fewer hyperparameters than deep learning, such as deep belief networks. Similar to SVM, the RBF kernel was applied in this study and the hyperparameters of the regulation coefficient (Cr) and kernel parameter (Kp) were optimised.

2.4. Inversion of the radiative transfer model

The PROSPECT model, which is based on the plate model (Allen *et al.* 1969), simulates leaf reflectance and transmittance. The first version was expressed as a function of three input parameters, including the internal structure parameter of the leaf mesophyll (N), chlorophyll content and water content. The input parameters of the latest version (PROSPECT-D) are leaf mass per area, brown pigments, carotenoid and anthocyanin contents, plus the above three parameters. Féret et al (2017) reported that PROSPECT-D outperforms all previous versions.

The model inversion of PROSPECT-D was conducted using MATLAB and Statistics Toolbox Release 2016a and the source codes (PROSPECT-D_Matlab.rar) downloaded from the portal site (Institut de physique du globe de Paris, 2017). The code for the inversion of PROSPECT-5 was modified for the application of PROSPECT-D. The absorption coefficients of this model were calibrated to avoid potential systematic bias and error propagation in the inversion process following Féret et al. (2008).

2.5. Performance assessment

All measurements were divided into three groups, training (50%), validation (25%) and test data (25%) for assessing the potential of machine learning algorithms (Hastie *et al.* 2009). To apply this strategy, all measurements were divided into four groups based on the shading treatments and, 50% of the groups were selected as training data, which were used for generating regression models, based on random number for each group. Next, 50% of the remaining measurements were selected as validation data, which were used for optimising hyperparameters of the machine learning algorithms. Finally, the last group was used as test data for evaluating accuracies. This procedure was repeated ten times to increase the robustness of the results.

After dividing the data, variable selection based on the genetic algorithm (GA), which is an adaptive heuristic search algorithm based on the evolutionary ideas of natural selection and genetics, was applied to remove non-informative variables to generate better and simpler prediction models (Villar *et al.* 2017) using the training data. This process was conducted using R 3.4.3 and the 'plsVarSel' package (Mehmood *et al*. 2012) and the preliminary parameters were set to the default values, which were proposed by Hasegawa *et al* (1999). Then, the hyperparameters of the regression models based on machine learning algorithms were optimised based on the estimation errors for the validation data.

For assessing vegetation indices, training data and validation data, sets were merged and used to generate regression models based on linear or exponential regression. This merged dataset was also used to calibrate the absorption coefficients of PROSPECT-D. Finally, chlorophyll contents were estimated for the test data and the accuracies of each model were evaluated based on them.

For evaluating performances, the ratio of performance to deviation (RPD, Equation (4)) (Williams 1987) was applied. Each method was classified into three categories based on RPD: Category 'A' (RPD > 2.0), Category 'B' (1.4 ≤ RPD ≤ 2.0) and Category 'C' (RPD < 1.4). Models classified as Categories 'A' or 'B' were assumed to have the potential to estimate chlorophyll content (Chang *et al.* 2001). Category 'A' is divided into three levels including approximate (2.0 ≤ RPD ≤ 2.5), good (2.5 < RPD ≤ 3.0) and excellent (RPD < 3.0) (Saeys *et al.* 2005).

$$\mathrm{RPD} = \mathrm{SD}/\mathrm{RMSE} \quad (4)$$

$$\mathrm{RMSE} = \sqrt{\frac{1}{n}\sum_{i=0}^{n}(\hat{y_i} - y_i)^2} \quad (5)$$

where SD is the standard deviation of the chlorophyll content in the test data, n is number of samples, y_i is the measured chlorophyll content and $\hat{y_i}$ is the estimated chlorophyll content.

A data-based sensitivity analysis (DSA) (Cortez and Embrechts 2013), which uses several training samples instead of a baseline vector and DSA has been applied for the regression or classification models based on machine learning algorithms by querying the fitted models with sensitivity samples, was applied for analysing the sensitivity of the regression models using R 3.4.3 and the ‘rminer’ package (Cortez and Embrechts 2013).

3. Results and Discussion

3.1. Chlorophyll content after each treatment

Chlorophyll a and b contents were determined based on measurements of the absorbance of the supernatant dimethyl-formamide extracts. Table 2 summarises the main characteristics of the measurements. The numbers of samples collected were not the same since some leaf disks were too thin to measure chlorophyll content using UV-1280. Figure 1 shows histograms of the chlorophyll content of the different shading treatments on the two dates. The mean values of chlorophyll content by leaf area ($\mu g/cm^2$) were 15.74, 23.37, 27.40 and 27.02 on 1 May, and 35.10, 44.79, 51.05 and 49.39 on 11 May for 0%, 35%, 75% and 90% shading, respectively.

Shading treatment makes leaf protein content higher and leaves become thicker (Poorter *et al.* 2006). So, shaded leaves contain more photosynthetic pigments, especially chlorophyll a, than sunlit leaves to harvest more light and nitrogen (Suzuki and Shioi 2003). As a result, the mean values of chlorophyll a and b contents were greater with more shading and a significant difference in chlorophyll content was confirmed among the four shading treatments when all the measurements from the two dates were combined ($p < 0.01$, based on ANOVA test). However, the differences in chlorophyll content were not significant for 35%, 75% or 90% shading for either date ($p < 0.05$, based on the Tukey-Kramer test) because the relative amount of chlorophyll b decreased and chlorophyll a/b ratios increased sharply in a linear manner at low light intensity (Leong and Anderson 1984).

<Table 2>

<Figure 1>

3.2. Spectral reflectance of different treatments

The reflected spectra of each shading treatment are presented in Figure 2. The reflectance of tea leaves near the green peak on 1 May was larger than that on 11 May and it was larger for lighter shading treatments. The red edge inflection points were confirmed around 740 nm as with previous studies (Vogelmann *et al.* 1993) and they became greater from 1 May to 11 May for all shading treatments, even though the differences in the reflectance at the start of the red edge (near 680 nm) were not significant among the four treatments. The differences in reflectance values between 800 nm and 1400 nm were unclear for 0% and 35% shading, while those of 75% and 90% shading on 11 May were apparently higher than those on 1 May. A similar trend was found in reflectance values of tea leaves between 1600 nm and 1800 nm.

<Figure 2>

For tea leaves, significant negative correlations were confirmed between chlorophyll content and reflectance values between 500 and 750 nm (Figure 3). The lowest correlations were obtained at 741 nm, 735 nm and 518 nm for all measurements acquired on 1 May and on 11 May, respectively.

<Figure 3>

3.3. Selected wavelengths based on GA

Table 3 lists the selected wavelengths for each round to estimate chlorophyll content based on GA.

The numbers of wavelengths were 10–16. Mainly, selected wavelengths were near the green peak and red edge inflection point of the tea leaves, and they were sensitive to chlorophyll content. However, some wavelengths shorter than 500 nm or greater than 750 nm, for which there were few differences in reflectance values among the four shading treatments, were selected and these values were used as references. These values have been applied to emphasise the reflectance at 680–690 nm for estimating total chlorophyll content in previous studies (Peñuelas *et al.* 1995b; Lichtenthaler *et al.* 1996).

<Table 3>

3.4. Selected indices based on GA

The indices, which were selected for estimating chlorophyll content based on GA, are listed in Table 4. From 3 to 6 indices were selected and used to reduce numbers of explanatory variables for regression models. MSAVI was selected three times; mSR2, TCI and EGFR were selected twice and most of the indices were selected only once. Chlorophyll strongly absorbs light at blue and red spectra and does not include light in green and orange spectra (Mattos *et al.* 2015). Most vegetation indices for chlorophyll content use wavelengths ranging from 400 to 860 nm. Furthermore, some stresses influence reflectance at specific wavelengths and reflectance between healthy and stressed vegetation can be detected in changes to the green peak and the red edge (Zarco-Tejada *et al.* 2001). As a result, some combinations consist of red edge-related indices and indices covering photosynthetically active radiation (PAR) domain.

<Table 4>

3.5. Accuracy validation

The statistical criteria of accuracies including the RPD, RMSE and R^2 from the test data are given in Table 5.

<Table 5>

Among all the machine learning algorithms with RPD values always greater than 2.0 when original reflectance values were used, KELM showed the best performance with RPD values of more than 3.38. This means that it is an excellent model for quantifying chlorophyll content. However, there is no advantage of using vegetation indices for machine learning regression and that made their RPD values smaller, except for round 2 and 9 of SVM. Rounds 4, 6 and 10 of SVM and round 6 of KELM were unacceptable as regression models for estimating chlorophyll contents.

Broadleaf trees are composed of two distinctive leaf groups of shaded and sunlit leaves and most of indices were divided into two groups including the sunlit leaf-oriented indices and the shaded-oriented indices (Sonobe and Wang 2017a). The light shading treatments, such as 0 % or 35 % shading, made sunlit leaves, while the heavy shading treatments, such as 75 % or 90% shading, made shaded leaves. As the result, few vegetation indices could be used as generally applicable indices to express the differences in leaf chlorophyll content and the combination of machine learning algorithms and vegetation indices led the worse results. The comparisons among the three algorithms were conducted based on the results of the original reflectance values.

To clarify which wavelengths were sensitive to their accuracies, a sensitivity analysis was conducted and Figure 4 shows the results of the DSA. Although there were specific differences in strategies in which wavelengths were attached weights to estimate chlorophyll contents, they were obscure between SVM and KELM and both used RBF kernel in this study, the accuracies of KELM were superior to those of SVM. Some previous studies showed the selection of the kernel function parameters can negatively affect their accuracies (Horvath 2003). The optimal values of σ ranged from 2^{-41} to 2^{-1} while Kp ranged from 2^{-8} to 2^{-2} based on Bayesian optimisation and that led the differences. (Huang *et al.* 2010) showed that the extreme learning machine has less optimisation constraints and its superiorities have been confirmed in regression (Maliha *et al.* 2018). The reflectance at 701–750 nm had the greatest influence on chlorophyll content estimations for all the algorithms; it occupied an importance of 45.1% for RF, while, no wavelength that occupied an importance of more than 20% was confirmed for SVM or KELM. Thus, RF achieved its high performances based on a few explanatory variables. This strategy might be effective than SVM; however, the red edge inflection points of tea leaves were increasing and the green peek was decreasing with the shading treatment (Figure 2). The excessive partialities of RF's importance made its estimation accuracies lower than KELM.

<Figure 4>

The RPD values of PROSPECT-D were relatively stable between 1.71 and 2.31; therefore, this method was assumed to have the potential to estimate chlorophyll content according to the criterion by Chang et al. (2001). In this model, the wavelength near the green peak and the red edge inflection point are not fully considered and the statistics of PROSPECT-D were inferior to those of the machine learning algorithms. However, it is useful to estimate other biochemical properties including carotenoid content, anthocyanin content, water content and leaf mass per area simultaneously. PROSPECT-D has a high potential for quantifying carotenoid content (Sonobe *et* *al.* 2018b). Since the chlorophyll to carotenoid ratio is an indicator for environmental stress in plants (Hendry and Price 1993), this model might be useful to assess physiological properties as well as biochemical properties. Furthermore, in some versions of PROSPECT, the influence of reflectance in total chlorophyll content is separated into chlorophyll a and b. However, a consideration of anthocyanin information and improvement in the measurement of individual photosynthetic pigment concentrations are needed since the measurement of carotenoid was not accurate enough (Zhang *et al.* 2017). Thus, there is some potential for using PROSPECT to assess vegetation properties following some improvements.

In this study, it was revealed that the combination of leaf scale spectroscopy and machine learning has exhibited relatively high accuracy and has been found to be useful for quick estimation of chlorophyll content. However, satellite- or unmanned aerial vehicle (UAV) remote sensing techniques are more of professional applications concerning large scale assessment. There remain many gaps to be crossed over from the study reported here to large scale satellite-borne applications.

4. Conclusions

The potential of vegetation reflectance for quantifying chlorophyll content of shaded tea was evaluated. In this study, two methods were assessed, the inversion of a radiative transfer model and machine learning algorithms, and the estimations based on machine learning algorithms were superior. Specifically, KELM yielded the most accurate estimation with a RMSE of 3.04 ± 0.52 μg cm^{-2} and RPD values from 3.38 to 5.92, which means the regression models based on KELM were excellent and were confirmed for quantifying chlorophyll content.

PROSPECT-D possessed some potential for this purpose; its RPD values ranged from 1.71 to 2.62 and more improvements were required to apply this method to shade grown tea cultivation. However, it is not sufficient to evaluate chlorophyll content of tea trees under high light stress and further improvements of the PROSPECT model are required. Our results showed that applying machine learning algorithms is a unique solution to conduct in-situ measurements of green tea.

Funding

This work was supported by the Science and Technology Research Promotion Program for Agriculture, Forestry, Fisheries, and Food Industry [grant number 27015C].

Disclosure statement

No potential conflicts of interest are reported by the authors.

References

Allen, WA, Gausman, HW, Richardson, AJ, Thomas, JR (1969) Interaction of isotropic light with a compact plant leaf. Journal of the Optical Society of America 59, 1376-1379.

Bergstra, J, Bengio, Y (2012) Random search for hyper-parameter optimization. Journal of Machine Learning Research 13, 281-305.

Biau, G, Scornet, E (2016) A random forest guided tour. Test 25, 197-227.

Blackburn, GA (1998a) Quantifying chlorophylls and caroteniods at leaf and canopy scales: An evaluation of some hyperspectral approaches. Remote Sensing of Environment 66, 273-285.

Blackburn, GA (1998b) Spectral indices for estimating photosynthetic pigment concentrations: a test using senescent tree leaves. International Journal of Remote Sensing 19, 657-675.

Blackburn, GA, Steele, CM (1999) Towards the remote sensing of matorral vegetation physiology: Relationships between spectral reflectance, pigment, and biophysical characteristics of semiarid bushland canopies. Remote Sensing of Environment 70, 278-292.

Boochs, F, Kupfer, G, Dockter, K, Kuhbauch, W (1990) Shape of the red edge as vitality indicator for plants. International Journal of Remote Sensing 11, 1741-1753.

Breiman, L (2001) Random forests. Machine Learning 45, 5-32.

Broge, NH, Leblanc, E (2001) Comparing prediction power and stability of broadband and hyperspectral vegetation indices for estimation of green leaf area index and canopy chlorophyll density. Remote Sensing of Environment 76, 156-172.

Buschmann, C, Nagel, E (1993) In vivo spectroscopy and internal optics of leaves as basis for remote sensing of vegetation. International Journal of Remote Sensing 14, 711-722.

Carter, GA (1994) Ratios of leaf reflectances in narrow wavebands as indicators of plant stress. International Journal of Remote Sensing 15, 697-703.

Carter, GA, Knapp, AK (2001) Leaf optical properties in higher plants: Linking spectral characteristics to stress and chlorophyll concentration. American Journal of Botany 88, 677-684.

Chang, CW, Laird, DA, Mausbach, MJ, Hurburgh, CR (2001) Near-infrared reflectance spectroscopy-principal components regression analyses of soil properties. Soil Science

Society of America Journal 65, 480-490.

Chappelle, EW, Kim, MS, McMurtrey, JE (1992) Ratio analysis of reflectance spectra (RARS): An algorithm for the remote estimation of the concentrations of chlorophyll A, chlorophyll B, and carotenoids in soybean leaves. Remote Sensing of Environment 39, 239-247.

Chatziantoniou, A, Petropoulos, GP, Psomiadis, E (2017) Co-Orbital Sentinel 1 and 2 for LULC Mapping with Emphasis on Wetlands in a Mediterranean Setting Based on Machine Learning. Remote Sensing 9,

Chemura, A, Mutanga, O, Odindi, J (2017) Empirical Modeling of Leaf Chlorophyll Content in Coffee (Coffea Arabica) Plantations With Sentinel-2 MSI Data: Effects of Spectral Settings, Spatial Resolution, and Crop Canopy Cover. IEEE Journal of Selected Topics in Applied Earth Observations and Remote Sensing 10, 5541-5550.

Chen, JM (1996) Evaluation of Vegetation Indices and a Modified Simple Ratio for Boreal Applications. Canadian Journal of Remote Sensing 22, 229-242.

Cho, MA, Skidmore, AK (2006) A new technique for extracting the red edge position from hyperspectral data: The linear extrapolation method. Remote Sensing of Environment 101, 181-193.

Collins, W (1978) Remote sensing of crop type and maturity. Photogrammetric Engineering and Remote Sensing 44, 43-55.

Cortez, P, Embrechts, MJ (2013) Using sensitivity analysis and visualization techniques to open black box data mining models. Information Sciences 225, 1-17.

Das, B, Sahoo, RN, Pargal, S, Krishna, G, Verma, R, Chinnusamy, V, Sehgal, VK, Gupta, VK (2017) Comparison of different uni- and multi-variate techniques for monitoring leaf water status as an indicator of water-deficit stress in wheat through spectroscopy. Biosystems Engineering 160, 69-83.

Dash, J, Curran, PJ (2004) The MERIS terrestrial chlorophyll index. International Journal of Remote Sensing 25, 5403-5413.

Datt, B (1998) Remote sensing of chlorophyll a, chlorophyll b, chlorophyll a+b, and total carotenoid content in eucalyptus leaves. Remote Sensing of Environment 66, 111-121.

Datt, B (1999a) A new reflectance index for remote sensing of chlorophyll content in higher plants: Tests using Eucalyptus leaves. Journal of Plant Physiology 154, 30-36.

Datt, B (1999b) Visible/near infrared reflectance and chlorophyll content in Eucalyptus leaves. International Journal of Remote Sensing 20, 2741-2759.

Daughtry, CST, Walthall, CL, Kim, MS, de Colstoun, EB, McMurtrey, JE (2000) Estimating corn leaf chlorophyll concentration from leaf and canopy reflectance. Remote Sensing of Environment 74, 229-239.

De Costa, WAJM, Mohotti, AJ, Wijeratne, MA (2007) Ecophysiology of tea. Brazilian Journal of Plant Physiology 19, 299-332.

Delalieux, S, Somers, B, Verstraeten, WW, Van Aardt, JAN, Keulemans, W, Coppin, P (2009) Hyperspectral indices to diagnose leaf biotic stress of apple plants, considering leaf phenology. International Journal of Remote Sensing 30, 1887-1912.

Ding, SF, Shi, ZZ, Tao, DC, An, B (2016) Recent advances in Support Vector Machines. Neurocomputing 211, 1-3.

Elarab, M, Ticlavilca, AM, Torres-Rua, AF, Maslova, I, McKee, M (2015) Estimating chlorophyll with thermal and broadband multispectral high resolution imagery from an unmanned aerial system using relevance vector machines for precision agriculture. International Journal of Applied Earth Observation and Geoinformation 43, 32-42.

Elvidge, CD, Chen, ZK (1995) Comparison of broad-band and narrow-band red and near-infrared vegetation indices. Remote Sensing of Environment 54, 38-48.

Filella, I, Amaro, T, Araus, JL, Peñuelas, J (1996) Relationship between photosynthetic radiation-use efficiency of Barley canopies and the photochemical reflectance index (PRI). Physiologia Plantarum 96, 211-216.

Filella, I, Serrano, L, Serra, J, Peñuelas, J (1995) Evaluating Wheat Nitrogen Status with Canopy Reflectance Indices and Discriminant Analysis. Crop Science 35, 1400-1405.

Féret, J-B, Francois, C, Asner, GP, Gitelson, AA, Martin, RE, Bidel, LPR, Ustin, SL, le Maire, G, Jacquemoud, S (2008) PROSPECT-4 and 5: Advances in the leaf optical properties model separating photosynthetic pigments. Remote Sensing of Environment 112, 3030-3043.

Féret, J-B, Gitelson, AA, Noble, SD, Jacquemoud, S (2017) PROSPECT-D: Towards modeling leaf optical properties through a complete lifecycle. Remote Sensing of Environment 193, 204-215.

Gabriel, JL, Zarco-Tejada, PJ, Lopez-Herrera, PJ, Perez-Martin, E, Alonso-Ayuso, M, Quemada, M (2017) Airborne and ground level sensors for monitoring nitrogen status in a maize crop. Biosystems Engineering 160, 124-133.

Gamon, JA, Surfus, JS (1999) Assessing leaf pigment content and activity with a reflectometer. New Phytologist 143, 105-117.

Gandia, S, Fernandez, G, Moreno, J (2005) 'Retrieval of Vegetation Biophysical Variables from CHRIS/PROBA Data in the SPARC Campaign, the 2nd CHRIS/Proba Workshop.' Frascati, Italy. (ESA/ESRIN:

Gitelson, A, Merzlyak, MN (1994) Spectral Reflectance Changes Associated with Autumn Senescence of Aesculus hippocastanum L. and Acer platanoides L. Leaves. Spectral Features and Relation to Chlorophyll Estimation. Journal of Plant Physiology 143, 286-292.

Gitelson, AA, Buschmann, C, Lichtenthaler, HK (1999) The chlorophyll fluorescence ratio F-735/F-700 as an accurate measure of the chlorophyll content in plants. Remote Sensing of Environment 69, 296-302.

Gitelson, AA, Gritz, Y, Merzlyak, MN (2003) Relationships between leaf chlorophyll content and spectral reflectance and algorithms for non-destructive chlorophyll assessment in higher plant leaves. Journal of Plant Physiology 160, 271-282.

Gitelson, AA, Kaufman, YJ, Merzlyak, MN (1996) Use of a green channel in remote sensing of global vegetation from EOS-MODIS. Remote Sensing of Environment 58, 289-298.

Gitelson, AA, Keydan, GP, Merzlyak, MN (2006) Three-band model for noninvasive estimation of chlorophyll, carotenoids, and anthocyanin contents in higher plant leaves. Geophysical Research Letters 33,

Gitelson, AA, Merzlyak, MN (1996) Signature analysis of leaf reflectance spectra: Algorithm development for remote sensing of chlorophyll. Journal of Plant Physiology 148, 494-500.

Gobron, N, Pinty, B, Verstraete, MM, Widlowski, JL (2000) Advanced vegetation indices optimized for up-coming sensors: Design, performance, and applications. IEEE Transactions on Geoscience and Remote Sensing 38, 2489-2505.

Gong, Z, Zhao, Y, Zhao, W, Lin, C (2014) Estimation model for plant leaf chlorophyll content based on the spectral index content. Acta Ecologica Sinica (in Chinese) 34, 5736-5745.

Guan, L, Liu, X (2009) Hyperspectral recognition models for physiological ecology characterization of rice in Cd pollution stress. Ecology and Environmental Sciences (in Chinese) 18, 488-493.

Guyot, G, Baret, F TDGaJJ Hunt (Ed.) (1988) 'Utilisation de la haute resolution spectrale pour suivre l'etat des couverts vegetaux, Spectral Signatures of Objects in Remote Sensing.' Aussois (Modane), France. (European Space Agency:

Haboudane, D, Miller, JR, Tremblay, N, Zarco-Tejada, PJ, Dextraze, L (2002) Integrated narrow-band vegetation indices for prediction of crop chlorophyll content for application to precision agriculture. Remote Sensing of Environment 81, 416-426.

Hasegawa, K, Kimura, T, Funatsu, K (1999) GA Strategy for Variable Selection in QSAR Studies: Application of GA-Based Region Selection to a 3D-QSAR Study of Acetylcholinesterase Inhibitors. Journal of Chemical Information and Computer Sciences 39, 112-120.

Hastie, T, Tibshirani, R, Friedman, J (Eds P Bickel, P Diggle, SE Fienberg, U Gather, S Zeger (2009) 'The Elements of Statistical Learning: Data Mining, Inference, and Prediction. Second Edition.' (Springer-Verlag New York: The United States)

Hendry, GAF, Price, AH (1993) 'Stress Indicators: Chlorophylls and Carotenoids.'

Hernandez-Clemente, R, Navarro-Cerrillo, RM, Zarco-Tejada, PJ (2014) Deriving Predictive Relationships of Carotenoid Content at the Canopy Level in a Conifer Forest Using Hyperspectral Imagery and Model Simulation. IEEE Transactions on Geoscience and Remote Sensing 52, 5206-5217.

Horler, DNH, Dockray, M, Barber, J (1983) The red edge of plant leaf reflectance. International

Journal of Remote Sensing 4, 273-288.

Horvath, G (2003) CMAC neural network as an SVM with B-spline kernel functions, 20th IEEE Instrumentation and Measurement Technology Conference, IMTC30, 1108-1113.

Hosgood, B, Jacquemoud, S, Andreoli, G, Verdebout, J, Pedrini, G, Schmuck, G (1994) Leaf Optical Properties EXperiment 93 (LOPEX93). European Commission, Joint Research Centre, Institute for Remote Sensing Applications. Report EUR 16095 EN, pp. 21.

Huang, GB, Ding, XJ, Zhou, HM (2010) Optimization method based extreme learning machine for classification. Neurocomputing 74, 155-163.

Huang, GB, Zhu, QY, Siew, CK (2006) Extreme learning machine: Theory and applications. Neurocomputing 70, 489-501.

Huete, A, Didan, K, Miura, T, Rodriguez, EP, Gao, X, Ferreira, LG (2002) Overview of the radiometric and biophysical performance of the MODIS vegetation indices. Remote Sensing of Environment 83, 195-213.

Hunt, ER, Daughtry, CST, Eitel, JUH, Long, DS (2011) Remote Sensing Leaf Chlorophyll Content Using a Visible Band Index. Agronomy Journal 103, 1090-1099.

Ishwaran, H (2015) The effect of splitting on random forests. Machine Learning 99, 75-118.

Jacquemoud, S, Ustin, SL, Verdebout, J, Schmuck, G, Andreoli, G, Hosgood, B (1996) Estimating leaf biochemistry using the PROSPECT leaf optical properties model. Remote Sensing of Environment 56, 194-202.

Japan Meteorological Agency (2017) https://www.jma.go.jp/jma/indexe.html

Jordan, CF (1969) Derivation of leaf area index from quality of light on the forest floor. Ecology 50, 663-666.

Karatzoglou, A, Smola, A, Hornik, K, Zeileis, A (2004) kernlab - An S4 Package for Kernel Methods in R. Journal of Statistical Software 11, 1-20.

Kim, MS, Daughtry, CST, Chappelle, EW, Mcmurtrey, JE, Walthall, CL (1994) 'The use high spectral resolution bands for estimating absorbed photo synthetically active radiation (APAR) 6th International Symposium on Physical Measurements and Signatures in Remote Sensing ' France.

Korus, A (2013) Effect of preliminary and technological treatments on the content of chlorophylls and carotenoids in kale (Brassica oleracea L. var. Acephala). Journal of Food Processing and Preservation 37, 335-344.

Kuriyama, S, Hozawa, A, Ohmori, K, Shimazu, T, Matsui, T, Ebihara, S, Awata, S, Nagatomi, R, Arai, H, Tsuji, I (2006) Green tea consumption and cognitive function: a cross-sectional study from the Tsurugaya Project. American Journal of Clinical Nutrition 83, 355-361.

le Maire, G, Francois, C, Dufrene, E (2004) Towards universal broad leaf chlorophyll indices using PROSPECT simulated database and hyperspectral reflectance measurements. Remote Sensing of Environment 89, 1-28.

le Maire, G, Francois, C, Soudani, K, Berveiller, D, Pontailler, J-Y, Breda, N, Genet, H, Davi, H, Dufrene, E (2008) Calibration and validation of hyperspectral indices for the estimation of broadleaved forest leaf chlorophyll content, leaf mass per area, leaf area index and leaf canopy biomass. Remote Sensing of Environment 112, 3846-3864.

Lee, LS, Choi, JH, Son, N, Kim, SH, Park, JD, Jang, DJ, Jeong, Y, Kim, HJ (2013) Metabolomic Analysis of the Effect of Shade Treatment on the Nutritional and Sensory Qualities of Green Tea. Journal of Agricultural and Food Chemistry 61, 332-338.

Leong, TY, Anderson, JM (1984) Adaptation of the thylakoid membranes of pea chloroplasts to light intensities. I. Study on the distribution of chlorophyll-protein complexes. Photosynthesis research 5, 105-15.

Li, XD, Mao, WJ, Jiang, W (2016) Multiple-kernel-learning-based extreme learning machine for classification design. Neural Computing & Applications 27, 175-184.

Li, ZH, Jin, XL, Wang, JH, Yang, GJ, Nie, CW, Xu, XG, Feng, HK (2015) Estimating winter wheat (Triticum aestivum) LAI and leaf chlorophyll content from canopy reflectance data by integrating agronomic prior knowledge with the PROSAIL model. International Journal of Remote Sensing 36, 2634-2653.

Liang, L, Qin, ZH, Zhao, SH, Di, LP, Zhang, C, Deng, MX, Lin, H, Zhang, LP, Wang, LJ, Liu, ZX (2016) Estimating crop chlorophyll content with hyperspectral vegetation indices and the hybrid inversion method. International Journal of Remote Sensing 37, 2923-2949.

Liaw, A, Wiener, M (2002) Classification and regression by random Forest. R News 2, 18-22.

Lichtenthaler, HK, Lang, M, Sowinska, M, Heisel, F, Miehe, JA (1996) Detection of vegetation stress via a new high resolution fluorescence imaging system. Journal of Plant Physiology 148, 599-612.

Maccioni, A, Agati, G, Mazzinghi, P (2001) New vegetation indices for remote measurement of chlorophylls based on leaf directional reflectance spectra. Journal of Photochemistry and Photobiology B-Biology 61, 52-61.

Main, R, Cho, MA, Mathieu, R, O'Kennedy, MM, Ramoelo, A, Koch, S (2011) An investigation into robust spectral indices for leaf chlorophyll estimation. Isprs Journal of Photogrammetry and Remote Sensing 66, 751-761.

Maliha, A, Yusof, R, Shapiai, MI (2018) Extreme learning machine for structured output spaces. Neural Computing & Applications 30, 1251-1264.

Masemola, C, Cho, MA, Ramoelo, A (2016) Comparison of Landsat 8 OLI and Landsat 7 ETM+ for estimating grassland LAI using model inversion and spectral indices: case study of Mpumalanga, South Africa. International Journal of Remote Sensing 37, 4401-4419.

Mattos, ER, Singh, M, Cabrera, ML, Das, KC (2015) Enhancement of biomass production in Scenedesmus bijuga high-density culture using weakly absorbed green light. Biomass & Bioenergy 81, 473-478.

McMurtrey, JE, Chappelle, EW, Kim, MS, Meisinger, JJ, Corp, LA (1994) Distinguishing nitrogen fertilization levels in field corn (Zea mays L.) with actively induced fluorescence and passive reflectance measurements. Remote Sensing of Environment 47, 36-44.

Mehmood, T, Liland, KH, Snipen, L, Sæbø, S (2012) A review of variable selection methods in Partial Least Squares Regression. Chemometrics and Intelligent Laboratory Systems 118, 62-69.

Miller, JR, Hare, EW, Wu, J (1990) Quantitative characterisation of the red edge reflectance 1. An inverted-Gaussian model. International Journal of Remote Sensing 11, 1755-1773.

Murchie, EH, Hubbart, S, Peng, S, Horton, P (2005) Acclimation of photosynthesis to high irradiance in rice: gene expression and interactions with leaf development. Journal of Experimental Botany 56, 449-460.

Mutanga, O, Skidmore, AK (2004) Narrow band vegetation indices overcome the saturation problem in biomass estimation. International Journal of Remote Sensing 25, 3999-4014.

Panda, SS, Ames, DP, Panigrahi, S (2010) Application of Vegetation Indices for Agricultural Crop

Yield Prediction Using Neural Network Techniques. Remote Sensing 2, 673-696.

Peñuelas, J, Filella, I, Gamon, JA (1995a) Assessment of photosynthetic radiation‐use efficiency with spectral reflectance. New Phytologist 131, 291-296.

Peñuelas, J, Filella, I, Lloret, P, Munoz, F, Vilajeliu, M (1995b) Reflectance assessment of mite effects on apple trees. International Journal of Remote Sensing 16, 2727-2733.

Peñuelas, J, Gamon, JA, Fredeen, AL, Merino, J, Field, CB (1994) Reflectance indices associated with physiological changes in nitrogen- and water-limited sunflower leaves. Remote Sensing of Environment 48, 135-146.

Poorter, H, Pepin, S, Rijkers, T, de Jong, Y, Evans, JR, Korner, C (2006) Construction costs, chemical composition and payback time of high- and low-irradiance leaves. Journal of Experimental Botany 57, 355-371.

Prado-Cabrero, A, Beatty, S, Howard, A, Stack, J, Bettin, P, Nolan, JM (2016) Assessment of lutein, zeaxanthin and meso-zeaxanthin concentrations in dietary supplements by chiral high-performance liquid chromatography. European Food Research and Technology 242, 599-608.

Qi, J, Chehbouni, A, Huete, AR, Kerr, YH, Sorooshian, S (1994) A modified soil adjusted vegetation index. Remote Sensing of Environment 48, 119-126.

R Core Team (2017). R: A language and environment for statistical computing. R Foundation for Statistical Computing, Vienna, Austria. https://www.R-project.org/.

Rondeaux, G, Steven, M, Baret, F (1996) Optimization of soil-adjusted vegetation indices. Remote Sensing of Environment 55, 95-107.

Roujean, JL, Breon, FM (1995) Estimating PAR absorbed by vegetation from bidirectional reflectance measurements. Remote Sensing of Environment 51, 375-384.

Saeys, W, Mouazen, AM, Ramon, H (2005) Potential for onsite and online analysis of pig manure using visible and near infrared reflectance spectroscopy. Biosystems Engineering 91, 393-402.

Shoko, C, Mutanga, O, Dube, T, Slotow, R (2018) Characterizing the spatio-temporal variations of C3 and C4 dominated grasslands aboveground biomass in the Drakensberg, South Africa. International Journal of Applied Earth Observation and Geoinformation 68, 51-60.

Sims, DA, Gamon, JA (2002) Relationships between leaf pigment content and spectral reflectance across a wide range of species, leaf structures and developmental stages. Remote Sensing of Environment 81, 337-354.

Smith, RCG, Adams, J, Stephens, DJ, Hick, PT (1995) Forecasting wheat yield in a Mediterranean-type environment from the NOAA satellite. Australian Journal of Agricultural Research 46, 113-125.

Snoek, J, Rippel, O, Swersky, K, Kiros, R, Satish, N, Sundaram, N, Patwary, MMA, Prabhat, Adams, RP F Bach, D Blei (Eds) (2015) 'Scalable Bayesian optimization using deep neural networks, the 32nd International Conference on Machine Learning (ICML).' Paris.

Sonobe, R, Miura, Y, Sano, T, H., H (2018a) Monitoring photosynthetic pigments of shade grown tea from hyperspectral reflectance. Canadian Journal of Remote Sensing

Sonobe, R, Miura, Y, Sano, T, Horie, H (2018b) Estimating leaf carotenoid contents of shade grown tea using hyperspectral indices and PROSPECT-D inversion. International Journal of Remote Sensing 39, 1306-1320.

Sonobe, R, Wang, Q (2018) Nondestructive assessments of carotenoids content of broadleaved plant species using hyperspectral indices Computers and Electronics in Agriculture 145, 18-26.

Sonobe, R, Wang, Q (2017a) Hyperspectral indices for quantifying leaf chlorophyll concentrations performed differently with different leaf types in deciduous forests. Ecological Informatics 37, 1-9.

Sonobe, R, Wang, Q (2017b) Towards a Universal Hyperspectral Index to Assess Chlorophyll Content in Deciduous Forests. Remote Sensing 9,

Sonobe, R, Yamaya, Y, Tani, H, Wang, XF, Kobayashi, N, Mochizuki, K (2017) Mapping crop cover using multi-temporal Landsat 8 OLI imagery. International Journal of Remote Sensing 38, 4348-4361.

Sonobe, R, Yamaya, Y, Tani, H, Wang, XF, Kobayashi, N, Mochizuki, K (2018c) Crop classification from Sentinel-2-derived vegetation indices using ensemble learning. Journal of Applied Remote Sensing 12,

Sun, J, Shi, S, Yang, J, Du, L, Gong, W, Chen, BW, Song, SL (2018) Analyzing the performance of PROSPECT model inversion based on different spectral information for leaf biochemical properties retrieval. Isprs Journal of Photogrammetry and Remote Sensing 135, 74-83.

Suzuki, Y, Shioi, Y (2003) Identification of chlorophylls and carotenoids in major teas by high-performance liquid chromatography with photodiode array detection. Journal of Agricultural and Food Chemistry 51, 5307-5314.

Terashima, I, Hikosaka, K (1995) Comparative ecophysiology of leaf and canopy photosynthesis. Plant Cell and Environment 18, 1111-1128.

Tucker, CJ (1979) Red and photographic infrared linear combinations for monitoring vegetation.

Remote Sensing of Environment 8, 127?150.

Villar, A, Vadillo, J, Santos, JI, Gorritxategi, E, Mabe, J, Arnaiz, A, Fernandez, LA (2017) Cider fermentation process monitoring by Vis-NIR sensor system and chemometrics. Food Chemistry 221, 100-106.

Vincini, M, Frazzi, E, D'Alessio, P (2008) A broad-band leaf chlorophyll vegetation index at the canopy scale. Precision Agriculture 9, 303-319.

Vincini, M, Frazzi, E, D’Alessio, P (2006) 'Angular dependence of maize and sugar beet VIs from directional CHRIS/Proba data, the 4th ESA CHRIS PROBA Workshop.'

Vogelmann, JE, Rock, BN, Moss, DM (1993) Red edge spectral measurements from sugar maple leaves. International Journal of Remote Sensing 14, 1563-1575.

Wang, KB, Liu, F, Liu, ZH, Huang, JA, Xu, ZX, Li, YH, Chen, JH, Gong, YS, Yang, XH (2010) Analysis of chemical components in oolong tea in relation to perceived quality. International Journal of Food Science and Technology 45, 913-920.

Wang, LF, Park, SC, Chung, JO, Baik, LH, Park, SK (2004) The compounds contributing to the greenness of green tea. Journal of Food Science 69, S301-S305.

Wellburn, AR (1994) The spectral determination of chlorophyll a and chlorophyll b, as well as total carotenoids, using various solvents with spectrophotometers of different resolution. Journal of Plant Physiology 144, 307-313.

Whetton, RL, Hassall, KL, Waine, TW, Mouazen, AM (2018) Hyperspectral measurements of yellow rust and fusarium head blight in cereal crops: Part 1: Laboratory study. Biosystems Engineering 166, 101-115.

Williams, P (1987) Variables affecting near-infraredreflectance spectroscopic analysis. In 'Near-

Infrared Technology in the Agricultural and Food Industries.' (Eds P Williams, K Norris.) pp. 143-167. (American Association of Cereal Chemists Inc.:

Wu, C, Niu, Z, Tang, Q, Huang, W (2008) Estimating chlorophyll content from hyperspectral vegetation indices: Modeling and validation. Agricultural and Forest Meteorology 148, 1230-1241.

Wu, CY, Niu, Z, Tang, Q, Huang, WJ, Rivard, B, Feng, JL (2009) Remote estimation of gross primary production in wheat using chlorophyll-related vegetation indices. Agricultural and Forest Meteorology 149, 1015-1021.

Yamamoto, A, Nakamura, T, Adu-Gyamfi, JJ, Saigusa, M (2002) Relationship between chlorophyll content in leaves of sorghum and pigeonpea determined by extraction method and by chlorophyll meter (SPAD-502). Journal of Plant Nutrition 25, 2295-2301.

Yan, Y (2016) 'Bayesian Optimization of Hyperparameters.' Available at

Zarco-Tejada, PJ, Berni, JAJ, Suarez, L, Sepulcre-Canto, G, Morales, F, Miller, JR (2009) Imaging chlorophyll fluorescence with an airborne narrow-band multispectral camera for vegetation stress detection. Remote Sensing of Environment 113, 1262-1275.

Zarco-Tejada, PJ, Miller, JR, Haboudane, D, Tremblay, N, Apostol, S (2003a) Detection of chlorophyll fluorescence in vegetation from airborne hyperspectral CASI imagery in the red edge spectral region. IGARSS 2003: IEEE International Geoscience and Remote Sensing Symposium, Vols I - Vii, Proceedings: Learning from Earth's Shapes and Sizes 598-600.

Zarco-Tejada, PJ, Miller, JR, Haboudane, D, Tremblay, N, Apostol, S (2003b) Detection of chlorophyll fluorescence in vegetation from airborne hyperspectral CASI imagery in the red edge spectral region. IGARSS 2003: IEEE International Geoscience and Remote Sensing Symposium, Vols I - Vii, Proceedings: Learning from Earth's Shapes and Sizes 598-600.

Zarco-Tejada, PJ, Miller, JR, Noland, TL, Mohammed, GH, Sampson, PH (2001) Scaling-up and model inversion methods with narrowband optical indices for chlorophyll content estimation in closed forest canopies with hyperspectral data. IEEE Transactions on Geoscience and Remote Sensing 39, 1491-1507.

Zarco-Tejada, PJ, Pushnik, JC, Dobrowski, S, Ustin, SL (2003c) Steady-state chlorophyll a fluorescence detection from canopy derivative reflectance and double-peak red-edge effects. Remote Sensing of Environment 84, 283-294.

Zhang, Y, Huang, JF, Wang, FM, Blackburn, GA, Zhang, HKK, Wang, XZ, Wei, CW, Zhang, KY, Wei, C (2017) An extended PROSPECT: Advance in the leaf optical properties model separating total chlorophylls into chlorophyll a and b. Scientific Reports 7, 10.

Zhao, J, Feng, M, Wang, C, Yang, W, Li, Z, Zhu, Z, Ren, P, Liu, T, Wang, H (2014) Simulating the Content of Chlorophyll in Winter Wheat Based on Spectral Vegetation Index. Journal of Shanxi Agricultural University (in Chinese) 34

Tables

Table 1 Vegetation indices evaluated in this study. dG: maximum of the first derivative of reflectance in the green, dRE: maximum of the first derivative of reflectance in the red edge

Index	Formula	Reference
Chlorophyll absorption ratio index (CARI)	R_{700}*(SQRT((a*670+R_{670}+b)^2))/R_{670}*(a^2+1)$^{0.5}$ a = (R_{700}–R_{550})/150 and b = R_{550}–(a*550)	(Kim *et al.* 1994)
Chlorophyll absorption ratio index 2 (CARI2)	(|(a+1)*R_{670}+b|/(a^2+1)$^{0.5}$)*(R_{700}/R_{670}) a = (R_{700}– R_{550})/150 and b = R_{550}–(a*550)	
Reflectance value at 550 nm (Carter)	R_{550}	(Carter and Knapp 2001)
Chl_{green}	$R_{NIR}/R_{GREEN}-1$ R_{NIR}: mean reflectance value from 760 to 800 nm R_{GREEN}: mean reflectance value from 540 to 560 nm	(Gitelson *et al.* 2006)
$Chl_{red\ edge}1$	$R_{NIR}/R_{RED\ EDGE}-1$ R_{NIR}: mean reflectance value from 760 to 800 nm $R_{RED\ EDGE}$: mean reflectance value from 690 to725 nm	
$Chl_{red\ edge}2$	$R_{750}/R_{710}-1$	(Wu *et al.* 2009)
Red-edge chlorophyll index (CI)	R_{675}* R_{690}/R_{683}^2	(Zarco-Tejada *et al.* 2009)
Chlorophyll vegetation index (CVI)	R_{NIR}*R_{RED}/R_{GREEN}^2 R_{GREEN}: mean reflectance value from 490 to 570 nm R_{RED}: mean reflectance value from 640 to 760 nm R_{NIR}: mean reflectance value from 780 to 1400 nm	(Vincini *et al.* 2008; Hunt *et al.* 2011)
D_{703}	D_{703}	(Boochs *et al.* 1990)
D_{720}	D_{720}	
Datt1	R_{860}/(R_{550}*R_{708})	(Datt 1998)
Datt2	R_{672}/(R_{550}*R_{708})	
Datt3	R_{672}/R_{550}	
Datt4	D_{754}/D_{704}	(Datt 1999b)
Datt5	R_{850}/R_{710}	(Datt 1999a)

Datt6	$(R_{850}–R_{710})/(R_{850}–R_{680})$	
Double difference (DD)	$(R_{749}–R_{720})–(R_{701}–R_{672})$	(le Maire *et al.* 2008)
DDn	$2*R_{710}–R_{(710–50)}–R_{(710+50)}$	(le Maire *et al.* 2008)
dND(522, 728)	$(D_{522}–D_{728})/(D_{522}+D_{728})$	(Sonobe and Wang 2017b)
Double-peak index (DPI)	$(D_{688}*D_{710})/D_{697}^2$	(Zarco-Tejada *et al.* 2003b)
dSR1	D_{730}/D_{706}	
dSR2	D_{705}/D_{722}	
DR(800, 550)	$R_{800}–R_{550}$	(Buschmann and Nagel 1993)
DR(800, 680)	$R_{800}–R_{680}$	(Jordan 1969)
Edge-green first derivative normalized difference (EGFN)	(dRE–dG)/(dRE+dG)	(Peñuelas *et al.* 1994)
Edge-green first derivative ratio (EGFR)	dRE/dG	
Enhanced vegetation index (EVI)	$2.5*((R_{800}–R_{670})/(R_{800}–(6*R_{670})–(7.5*R_{475}) + 1))$	(Huete *et al.* 2002)
First derivative normalized difference vegetation index (FDNDVI)	$(D_{630}–D_{723})/(D_{630}+D_{723})$	(Zhao *et al.* 2014)
Greenness index (GI)	R_{554}/R_{677}	(Smith *et al.* 1995)
Gitel1	$1/R_{700}$	(Gitelson *et al.* 1999)
Gitel2	$(R_{750}–R_{800}/R_{695}–R_{740})–1$	(Gitelson *et al.* 2003)
Global imager vegetation index (GLI)	$(2*R_{GREEN}–R_{RED}–R_{BLUE})/ (2* R_{GREEN} + R_{RED} + R_{BLUE})$ R_{BLUE}: mean reflectance value from 420 to 480 nm R_{GREEN}: mean reflectance value from 490 to 570 nm R_{RED}: mean reflectance value from 640 to 760 nm	(Gobron *et al.* 2000)
Green normalized difference vegetation index	$(R_{800}–R_{550})/(R_{800}+R_{550})$	(Gitelson *et al.* 1996)

(GNDVI)		
Mac	$(R_{780}-R_{710})/(R_{780}-R_{680})$	(Maccioni *et al.* 2001)
Modified chlorophyll absorption in reflectance index (MCARI)	$((R_{700}-R_{670})-0.2*(R_{700}-R_{550}))*(R_{700}/R_{670})$	(Daughtry *et al.* 2000)
MCARI/OSAVI	MCARI/OSAVI	
Modified chlorophyll absorption in reflectance index 1 (MCARI1)	$1.5[1.2(R_{712}-R_{670})-0.5(R_{712}-R_{550})](R_{712}/R_{670})$	(Guan and Liu 2009)
MCARI1/MSAVI	MCARI1/MSAVI	
Modified chlorophyll absorption in reflectance index 2 (MCARI2)	$((R_{750}-R_{705})-0.2*(R_{750}-R_{550}))*(R_{750}/R_{705})$	(Wu *et al.* 2008)
MCARI2/OSAVI2	MCARI2/OSAVI2	(Wu *et al.* 2008)
mND705	$(R_{750}-R_{705})/(R_{750}+R_{705}-2R_{445})$	(Sims and Gamon 2002)
mNDVI	$(R_{800}-R_{680})/(R_{800}+R_{680}-2R_{445})$	
mREIP	The index based on the Gaussian fit of the red edge derivative	(Miller *et al.* 1990)
Modified soil adjusted vegetation index (MSAVI)	$0.5*(2*R_{800}+1-SQRT((2*R_{800}+1)^2-8*(R_{800}-R_{670})))$	(Qi *et al.* 1994)
mSR1	$(R_{750}-R_{445})/(R_{705}-R_{445})$	(Sims and Gamon 2002)
mSR2	$(R_{800}-R_{445})/(R_{680}-R_{445})$	
mSR3	$(R_{750}/R_{705}-1)/SQRT((R_{750}/R_{705})+1)$	(Chen 1996)
MERIS terrestrial chlorophyll index (MTCI)	$(R_{754}-R_{709})/(R_{709}-R_{681})$	(Dash and Curran 2004)
Modified triangular vegetation index (MTVI)	$1.5[1.2(R_{712}-R_{550})-2.1(R_{670}-R_{550})]$	(Guan and Liu 2009)
MTVI/MSAVI	MTVI/MSAVI	
ND	$(R_{565}-R_{735})/(R_{565}+R_{735})$	(Gong *et al.* 2014)
Normalized difference	$(R_{800}-R_{670})/(R_{800}+R_{670})$	(Tucker 1979)

vegetation index 1 (NDVI1)		
Normalized difference vegetation index 2 (NDVI2)	$(R_{750}-R_{705})/(R_{750}+R_{705})$	(Gitelson and Merzlyak 1994; Gamon and Surfus 1999)
Normalized difference vegetation index 3 (NDVI3)	$(R_{682}-R_{553})/(R_{682}+R_{553})$	(Gandia *et al.* 2005)
Normalized pigments reflectance index (NPCI)	$(R_{680}-R_{460})/(R_{680}+R_{460})$	(Blackburn 1998a, 1998b)
Normalized pigments reflectance index 2 (NPCI2)	$(R_{680}-R_{430})/(R_{680}+R_{430})$	(Peñuelas *et al.* 1994)
Optimized soil adjusted vegetation index (OSAVI)	$(1+0.16)*(R_{800}-R_{670})/(R_{800}+R_{670}+0.16)$	(Rondeaux *et al.* 1996)
Optimized soil adjusted vegetation index 2 (OSAVI2)	$(1+0.16)*(R_{750}-R_{705})/(R_{750}+R_{705}+0.16)$	(Wu *et al.* 2008)
Pigment specific normalized difference for chlorophyll a (PSNDa)	$(R_{800}-R_{680})/(R_{800}+R_{680})$	
Pigment specific normalized difference for chlorophyll b (PSNDb)	$(R_{800}-R_{635})/(R_{800}+R_{635})$	(Blackburn 1998a, 1998b)
Pigment specific simple ratio for chlorophyll a (PSSRa)	R_{800}/R_{680}	
Pigment specific simple ratio for chlorophyll b (PSSRb)	R_{800}/R_{635}	

Renormalized difference vegetation index (RDVI)	$(R_{800}-R_{670})/(SQRT(R_{800}+R_{670}))$	(Roujean and Breon 1995)
Wavelength of the red edge (RE)	Amplitude of the main peak in the first derivative of the reflectance spectra	(Filella *et al.* 1996)
Red-Edge Inflection Point (REIP)	The position of the red edge inflection point	(Collins 1978; Horler *et al.* 1983)
Red-edge position liner extrapolation method1 (REP1)	$700+40*((R_{re}-R_{700})/(R_{740}-R_{700}))$ $R_{re=}(R_{670}-R_{780})/2$	(Cho and Skidmore 2006)
Red-edge position liner extrapolation method2 (REP2)	$700+40*((R_{670}+R_{780})/2-R_{700})/(R_{740}-R_{700}))$	(Guyot and Baret 1988)
Structure intensive pigment index (SIPI)	$(R_{800}-R_{445})/(R_{800}-R_{680})$	(Peñuelas *et al.* 1995b)
Spectral polygon vegetation index (SPVI)	$0.4*3.7*(R_{800}-R_{670})-1.2*SQRT((R_{530}-R_{670})^2)$	(Vincini *et al.* 2006; Main *et al.* 2011)
SR1	R_{605}/R_{760}	
SR2	R_{695}/R_{760}	
SR3	R_{710}/R_{760}	(Carter 1994)
SR4	R_{695}/R_{420}	
SR5	R_{695}/R_{670}	
SR6	R_{675}/R_{700}	(Chappelle *et al.* 1992)
SR7	R_{750}/R_{550}	(Gitelson and Merzlyak 1996)
SR8	R_{750}/R_{700}	
SR9	R_{752}/R_{690}	
SR10	R_{440}/R_{690}	(Lichtenthaler *et al.* 1996)
SR11	R_{700}/R_{670}	(McMurtrey *et al.* 1994)
SR12	R_{430}/R_{680}	(Peñuelas *et al.* 1995a)
SR13	R_{740}/R_{720}	(Vogelmann *et al.* 1993)
SR14	R_{750}/R_{710}	(Zarco-Tejada *et al.* 2003c)
SR15	R_{565}/R_{740}	(Gong *et al.* 2014)
SR16	R_{1250}/R_{1050}	(Delalieux *et al.* 2009)
SRC	R_{800}/R_{680}	(Jordan 1969)
Sum of the	The sum of the amplitudes between 680 and	(Filella *et al.* 1995)

amplitudes between 680 and 780 nm in the first derivative of the reflectance spectra (Sum1)	780 nm in the first derivative of the reflectance spectra	
Sum of derivative values between 626 nm and 795 nm (Sum2)	The sum of derivative values between 626 nm and 795 nm.	(Elvidge and Chen 1995)
Transformed chlorophyll absorption ratio (TCARI)	$3*((R_{700}–R_{670})–0.2*(R_{700}–R_{550})*(R_{700}/R_{670}))$	(Haboudane *et al.* 2002)
TCARI/OSAVI	TCARI/OSAVI	
Transformed chlorophyll absorption ratio 2 (TCARI2)	$3*((R_{750}–R_{705})–0.2*(R_{750}–R_{550})*(R_{750}/R_{705}))$	(Wu *et al.* 2008)
TCARI2/OSAVI2	TCARI2/OSAVI2	
Triangular chlorophyll index (TCI)	$1.2*(R_{700}–R_{550})–1.5*(R_{670}–R_{550})*SQRT(R_{700}/R_{670})$	(Hunt *et al.* 2011)
Transformed vegetation index (TVI)	$0.5*(120*(R_{750}–R_{550})–200*(R_{670}–R_{550}))$	(Broge and Leblanc 2001)
Voge1	D_{715}/D_{705}	(Vogelmann *et al.* 1993)
Voge2	$(R_{734}–R_{747})/(R_{715}+R_{726})$	

Table 2 Main characteristics of the measurements in this study.

Shading	0%		35%		75%		90%	
Date	01 May	11 May	01 May	11 May	01 May	11 May	01 May	11 May
Number of samples	8	15	12	15	12	15	14	15
Minimum	9.24	24.58	16.84	36.20	19.62	36.41	17.03	29.63
1st Quartile	13.06	31.42	19.03	40.78	24.11	49.39	21.88	46.73
Median	16.01	33.64	22.42	44.28	26.16	51.27	27.02	49.30
Mean	15.74	35.10	23.37	44.79	27.40	51.05	26.77	49.39
3rd Quartile	18.72	38.35	27.21	46.93	30.46	55.01	32.61	54.99
Maximum	21.63	46.25	31.75	55.80	38.51	57.89	38.04	60.60

Table 3. Selected wavelengths (nm) based on GA.

Round	Wavelength (nm)
1	481, 494, 541, 544, 564, 582, 618, 630, 634, 664, 730, 770, 771
2	409, 426, 513, 520, 546, 553, 574, 576, 586, 606, 657, 681, 689, 702, 745, 753
3	535, 556, 565, 571, 609, 612, 620, 643, 650, 736, 755, 766, 768
4	410, 520, 526, 534, 572, 573, 614, 618, 623, 639, 642, 713, 770, 772
5	434, 448, 528, 591, 599, 636, 677, 695, 697, 742, 749, 752, 763
6	401, 419, 432, 492, 625, 648, 672, 677, 706, 736, 737, 749, 777
7	443, 450, 453, 495, 497, 569, 587, 646, 648, 677, 689, 739
8	415, 423, 449, 485, 511, 526, 541, 545, 591, 605, 654, 655, 688, 704, 728, 776
9	427, 472, 485, 493, 518, 527, 546, 596, 602, 619, 659, 672, 675, 711, 728
10	441, 458, 461, 597, 679, 697, 703, 735, 747, 760

Table 4. Selected indices based on GA.

Round	Index
1	SR2, SR4, MCARI2
2	Datt1, EGFN, NPCI2, mSR2, TCI
3	Mac, D1, MSAVI, RDVI.1
4	PSSRb, SR6, SR14
5	EGFR, MSAVI, OSAVI2, GLI
6	EGFN, mSR2, SR3, GI, MTCI
7	mREIP, PSNDb, SR11, MCARI1, TCI
8	PSNDb, SR8, CI, DDn, DPI, RDVI
9	Datt4, Gitel1, MSAVI, D800_550
10	EGFR, NPCI, TVI

Table 5. Effective methods for quantifying chlorophyll content.

	Round 1			Round 2			Round 3			Round 4			Round 5		
	R^2	RMSE	RPD	R^2	RMSE	RPD	R^2	RMSE	RPD	R^2	RMSE	RPD	R^2	RMSE	RPD
Machine learning															
Reflectance															
SVM	0.77	4.66	2.46	0.94	3.64	3.87	0.87	4.32	2.83	0.82	5.65	2.36	0.96	2.84	4.32
RF	0.87	4.04	2.84	0.94	3.39	4.15	0.93	3.63	3.37	0.85	4.85	2.75	0.95	3.29	3.73
KELM	0.95	2.57	4.47	0.94	2.83	4.96	0.95	2.85	4.29	0.83	3.58	3.73	0.96	2.59	4.73
Vegetation index															
SVM	0.69	7.87	1.46	0.93	3.60	3.90	0.82	6.16	1.98	0.39	11.03	1.21	0.89	4.10	3.00
RF	0.76	5.51	2.08	0.81	6.08	2.31	0.88	4.24	2.88	0.68	7.66	1.74	0.77	5.99	2.05
KELM	0.92	3.22	3.56	0.95	3.25	4.32	0.74	6.32	1.94	0.67	7.60	1.76	0.83	4.97	2.47
Model inversion															
PROSPECT-D	0.69	6.71	1.71	0.79	6.87	2.05	0.77	6.30	1.94	0.72	7.45	1.79	0.81	6.41	1.91
	Round 6			Round 7			Round 8			Round 9			Round 10		
	R^2	RMSE	RPD	R^2	RMSE	RPD	R^2	RMSE	RPD	R^2	RMSE	RPD	R^2	RMSE	RPD
Machine learning															
Reflectance															
SVM	0.96	3.09	5.06	0.92	4.19	3.29	0.95	3.57	4.20	0.74	6.00	2.28	0.84	4.87	2.57
RF	0.96	3.49	4.48	0.95	3.12	4.42	0.90	4.86	3.08	0.88	4.70	2.91	0.94	3.97	3.15
KELM	0.97	2.65	5.92	0.93	2.82	4.89	0.94	3.75	4.00	0.92	4.05	3.38	0.96	2.66	4.70
Vegetation index															
SVM	0.69	14.50	1.08	0.62	8.70	1.58	0.52	10.33	1.45	0.84	5.71	2.40	0.51	11.80	1.06
RF	0.83	7.03	2.23	0.71	7.75	1.78	0.78	7.08	2.12	0.85	5.47	2.50	0.54	8.85	1.41
KELM	0.25	13.36	1.17	0.76	7.25	1.90	0.85	6.07	2.47	0.80	6.48	2.11	0.58	8.27	1.51
Model inversion															
PROSPECT-D	0.92	6.78	2.31	0.81	7.93	1.74	0.76	8.38	1.79	0.83	5.92	2.31	0.77	6.62	1.89

Figures

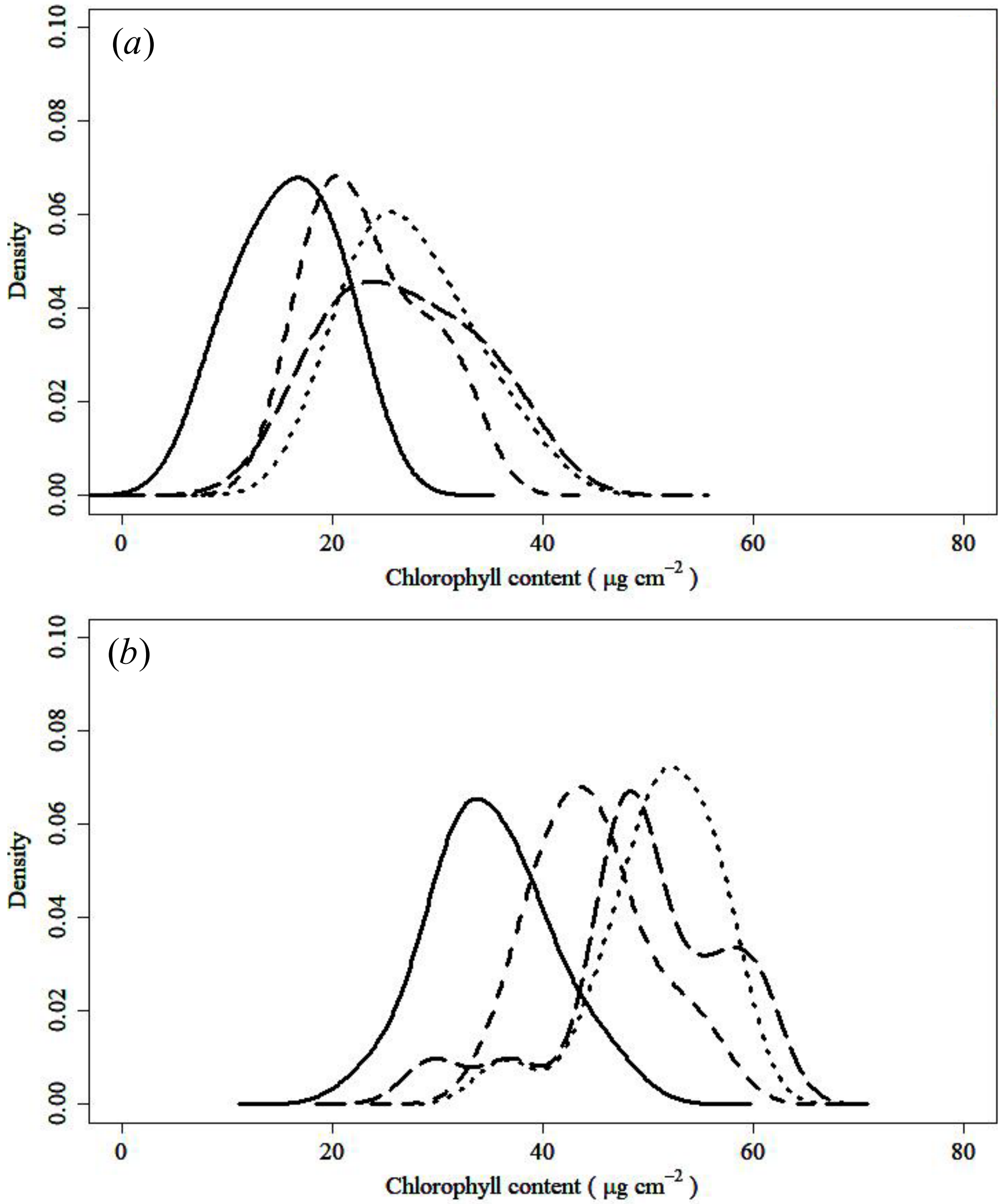

Figure 1. Histograms of chlorophyll content on (a) 1 May and (b) 11 May. Continuous, dashed, dotted and long dashed lines represent distributions of chlorophyll content after 0 %, 35 %, 75 % and 90 % shading, respectively.

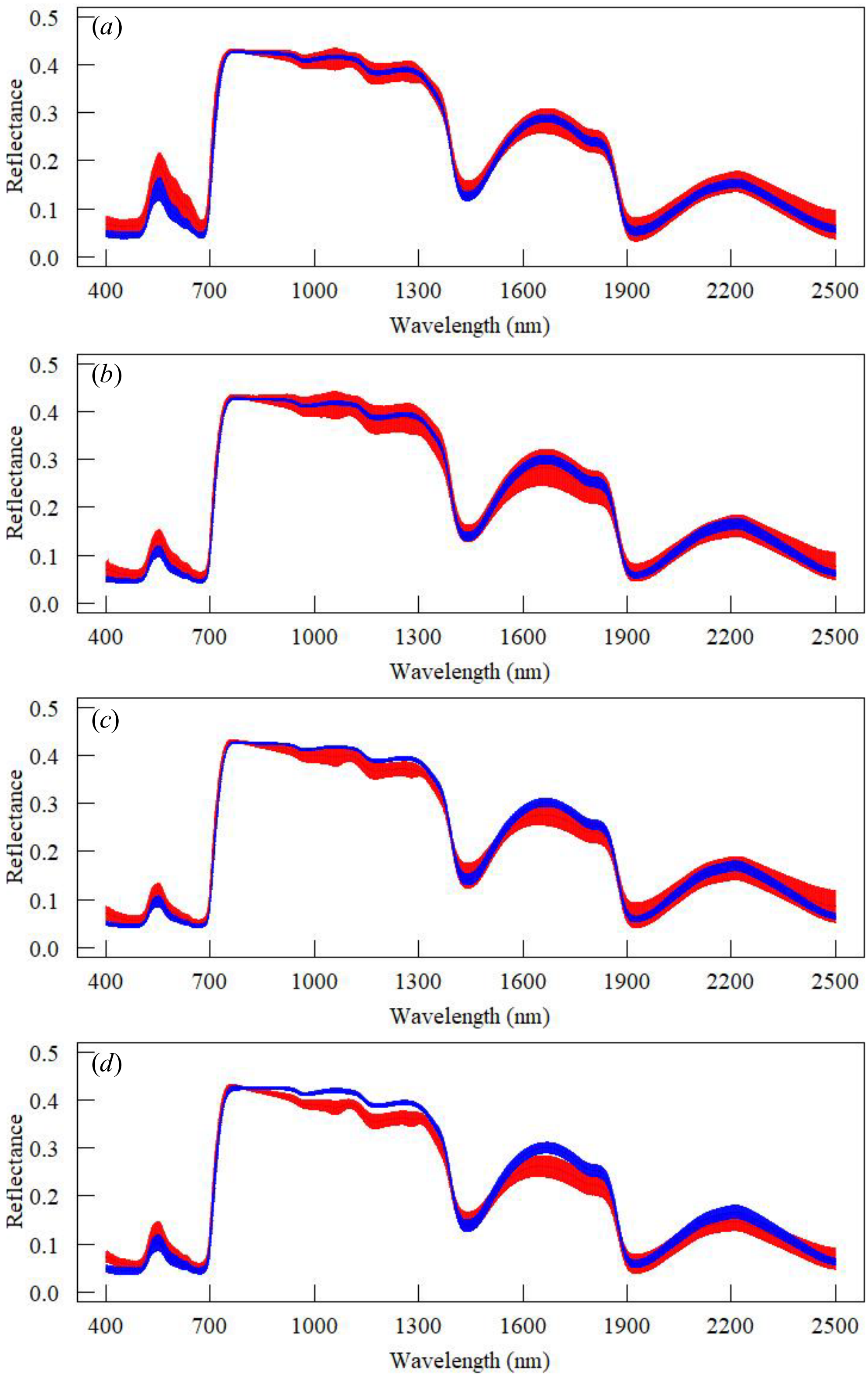

Figure 2. Mean reflectance spectra and standard deviations for (a) 0% shading, (b) 35% shading, (c)75% shading and (d) 90% shading. Red and blue represent measurements on 1 May and 11 May, respectively.

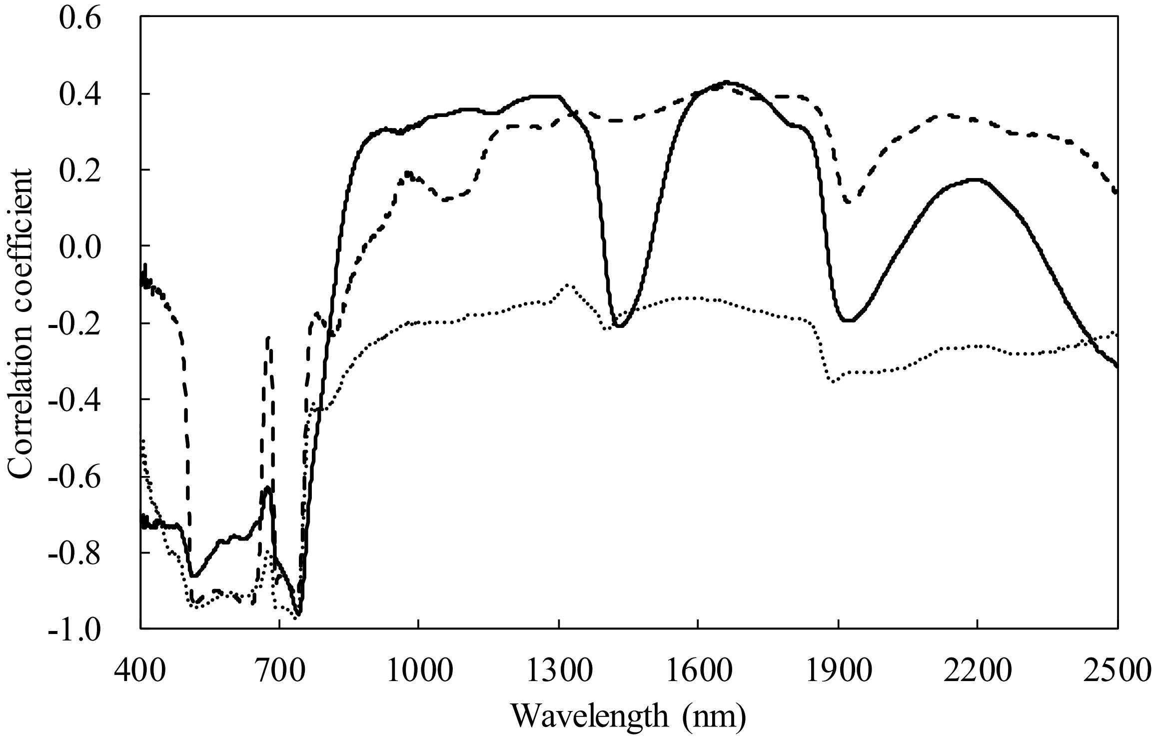

Figure 3. Correlations between reflectance and chlorophyll content. Continuous, dotted and broken lines represent correlation coefficients for all, on 1 May and on 11 May, respectively.

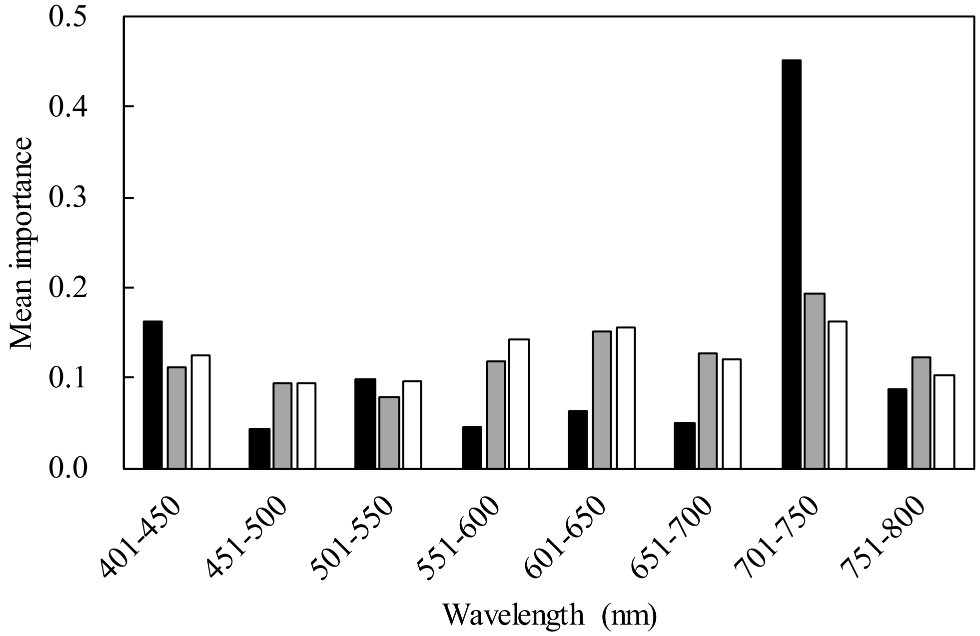

Figure 4. DSA results for RF (black), SVM (grey) and KELM(white). Importance values were averaged for ten repetitions.